American Journal of Materials Science 2014, 4(2): 45-55
DOI: 10.5923/j.materials.20140402.01

Plane Wave Propagation in a Rotating Polygonal Cross-sectional Plate Immersed in Fluid

P. Ponnusamy

Department of Mathematics, Government Arts College (Autonomous), Coimbatore, 641 018, Tamil Nadu, India

Abstract The free vibration of homogeneous, isotropic rotating plate of polygonal cross-section immersed in fluid is studied within the frame work of the linearized, two-dimensional plane theory of elasticity. The equations of motion of the plate are formulated using the constitutive equations of a isotropic material with preferred material direction collinear with the longitudinal axis of the plate. The equations of motion of the fluid are formulated using the constitutive equations of the inviscid fluid. Displacement potentials are used to solve the equations of motion of the plate and the fluid. The frequency equation of the coupled system consisting of the plate and fluid is developed under the assumption of perfect-slip boundary conditions at the solid-fluid interfaces. The non-dimensional frequencies of longitudinal and flexural antisymmetric modes of vibrations are obtained using the Fourier Expansion Collocation Method (FECM), and they are presented in the form of dispersion curves.

Keywords Solid-fluid interface, Wave propagation in plate, Vibration of thermal plate, Piezoelectric plate, Plate immersed in fluid, Generalized thermo elastic plate, Rotating cylinder/rotating plate

1. Introduction

The plates of circular and plates of polygonal cross-sections are often used as structural components and their vibration characteristics are important for practical design. The frequency responses of rotating arbitrary/ polygonal cross-sectional plates has many applications in various fields of science and technology, namely, submarine structures, pressure vessel, borewells, ship building industries and have many other engineering applications. Nagaya [1,2] studied the simplified method for solving problems of vibrating plates of doubly connected arbitrary shape using the Fourier expansion collocation method, he has detained the frequency equations for a doubly connected polygonal cross-sectional plate and numerical calculation were carried for the above said cross-sections. Following Nagaya, Ponnusamy [3, 4, 5] discussed the frequency responses of generalized thermo elastic cylinder and thermo-elastic plate of arbitrary cross-sections and generalized thermo-elastic plate of polygonal cross-sections by using the Fourier expansion collocation method developed by Nagaya [1,2]. Further the same author [6] investigated the wave propagation in a piezoelectric solid bar of circular cross-section immersed in fluid.

The effect of rotation on elastic waves in solids was studied by many authors, such as Clarke and Burdess [7], Wren and Burdess [8] and Soderkvist [9]. Ting [10] analyzed the interfacial waves in a rotating anisotropic elastic half space by extending the Stroh [11] formalism. He obtained explicit expression of the polarization vector and the secular equation for monoclinic material half space rotating about the normal to the plane of symmetry. Fang et al [12, 13] studied respectively the effect of rotation on the characteristic of wave propagation in a piezoelectric plate and the effect of rotation on surface acoustic waves in a piezoelectric half space. Sharma and Thakur [14] presented the effect of rotation on Rayleigh-Lamb waves in magneto-thermoelastic plates. Sharma and Othman [15] investigated the effect of rotation on generalized thermo viscoelastic Rayleigh-Lamb waves in plates. Walia et al. [16] studied the propagation characteristics of thermoelastic waves in piezoelectric (6mm class) rotating plate.

For fluid sensor application, vibration modes of an elastic body without normal displacement at its surface are ideal. When the body is vibrating in these modes no pressure waves are generated in the fluid. The fluid produces a drag on the body surface only due to the fluid and the tangential motion of the surface, therby lowering the frequencies of the waves may also cause additional dispersion. Both stationary waves in resonators and propagationg waves in wave guides have been used for fluid sensors. For example, face-shear, thickness-shear and thickness-twist modes in plates are widely used for fluid sensor applications. In these modes, motions of material particles are parallel to the surface of the plates. Understanding the behavior of these waves is

* Corresponding author:
ponnusamypp@yahoo.com (P. Ponnusamy)
Published online at http://journal.sapub.org/materials

fundamentally important to acoustic wave fluid sensors. Sun et al. [17] studied the sheat-horizontal waves in a rotated Y-cut quartz plate in contact with a viscous fluid.

Assaf et al [18] analyzed the vibration and acoustic responses of damped sandwich plates immersed in a light or heavy fluid. Three dimensional vibration analysis of an infinite poroelastic plate immersed in an inviscid elastic fluid was discussed by Ahmed Shah and Tajuddin [19].

Keeping these facts in view, an attempt has been made to investigate the free vibration analysis of rotating polygonal cross-sectional plate immersed in fluid, which has not been discussed by any researchers. The plate is assumed to be rotating with uniform angular velocity about its axis.

2. Formulation of the Problem

We consider a homogeneous, isotropic rotating elastic plate of polygonal cross-section. The system displacements and stresses are defined by the polar coordinates r and θ in an arbitrary point inside the plate and denote the displacements u_r in the direction of r and u_θ in the tangential direction θ. The in-plane vibration and displacements of rotating polygonal cross-sectional plate is obtained by assuming that there is no vibration and a displacement along the z axis in the cylindrical coordinate system (r,θ,z). The two dimensional stress equations of motion, strain –displacement relations in the absence of body forces for a linearly elastic medium are

$$\sigma_{rr,r}+r^{-1}\sigma_{r\theta,\theta}+r^{-1}\left(\sigma_{rr}-\sigma_{\theta\theta}\right)+\rho\Omega^2 u_r=\rho u_{r,tt}$$
$$\sigma_{r\theta,r}+r^{-1}\sigma_{\theta\theta,\theta}+2r^{-1}\sigma_{r\theta}=\rho u_{\theta,tt} \tag{1}$$

where

$$\sigma_{rr}=\lambda\left(e_{rr}+e_{\theta\theta}\right)+2\mu e_{rr}$$
$$\sigma_{\theta\theta}=\lambda\left(e_{rr}+e_{\theta\theta}\right)+2\mu e_{\theta\theta} \tag{2}$$
$$\sigma_{r\theta}=2\mu e_{r\theta}$$

where $\sigma_{rr,}\sigma_{\theta\theta,}\sigma_{r\theta}$ are the stress components, $e_{rr,}e_{\theta\theta,}e_{r\theta}$ are the strain components, ρ is the mass density, Ω^2 is the rotational speed, t is the time, λ and μ are Lame' constants.

The strain e_{ij} related to the displacements are given by

$$e_{rr}=u_{r,r},e_{\theta\theta}=r^{-1}\left(u_r+u_{\theta,\theta}\right),$$
$$e_{r\theta}=u_{\theta,r}-r^{-1}\left(u_\theta-u_{r,\theta}\right) \tag{3}$$

in which u_r and u_θ is the displacement components along radial and circumferential directions respectively. The comma in the subscripts denotes the partial differentiation with respect to the variables.

Substituting the Eqs. (3) and (2) in Eq. (1), the following displacement equations of motions are obtained as

$$(\lambda+2\mu)\left(u_{r,rr}+r^{-1}u_{r,r}-r^{-2}u_r\right)+\mu r^{-2}u_{r,\theta\theta}+r^{-1}(\lambda+\mu)u_{\theta,r\theta}+r^{-2}(\lambda+3\mu)u_{\theta,\theta}+\rho\Omega^2u_r=\rho u_{r,tt}$$
$$\mu\left(u_{\theta,rr}+r^{-1}u_{\theta,r}-r^{-2}u_\theta\right)+r^{-2}(\lambda+2\mu)u_{\theta,\theta\theta}+r^{-2}(\lambda+3\mu)u_{r,\theta}+r^{-1}(\lambda+\mu)u_{r,r\theta}=\rho u_{\theta,tt} \tag{4}$$

3. Solutions of Solid Medium

The Eq. (4) is a coupled partial differential equation with two displacements components. To uncouple the equation (4), we follow Mirsky [10] by assuming the vibration and displacements along the axial direction z equal to zero. Hence assuming the solutions of the Eq. (4) in the form

$$u_r(r,\theta,z,t)=\sum_{n=0}^{\infty}\varepsilon_n\left[\left(\phi_{n,r}+r^{-1}\psi_{n,\theta}\right)+\left(\overline{\phi}_{n,r}+r^{-1}\overline{\psi}_{n,\theta}\right)\right]e^{i\omega t}$$
$$u_\theta(r,\theta,z,t)=\sum_{n=0}^{\infty}\varepsilon_n\left[\left(r^{-1}\phi_{n,\theta}-\psi_{n,r}\right)+\left(r^{-1}\overline{\phi}_{n,\theta}-\overline{\psi}_{n,r}\right)\right]e^{i\omega t} \tag{5}$$

where $\varepsilon_n=\dfrac{1}{2}$ for $n=0$, $\varepsilon_n=1$ for $n\geq 1$, $i=\sqrt{-1}$, ω is the angular frequency, $\phi_n(r,\theta)$, $\psi_n(r,\theta)$, $\overline{\phi}_n(r,\theta)$, and $\overline{\psi}_n(r,\theta)$ are the displacement potentials.

By introducing the dimensionless quantities $\overline{\lambda} = (\lambda/\mu)$, $\xi^2 = \rho\omega^2 a^2/\mu$, $c^2 = \Omega^2\xi^2/\omega^2$, $\omega^* = \xi/a\sqrt{\mu/\rho}$, $T = t\sqrt{\mu/\rho}/a$, $x = r/a$, c^2 is the rotational velocity, and substituting Eq.(5) in Eq.(4), we obtain

$$\left[\left(2+\overline{\lambda}\right)\nabla^2 + \left(\xi^2 + c^2\right)\right]\phi_n = 0 \tag{6}$$

and

$$\left[\nabla^2 + \left(\xi^2 + c^2\right)\right]\psi_n = 0 \tag{7}$$

where $\nabla^2 \equiv \partial^2/\partial x^2 + x^{-1}\partial/\partial x + x^{-2}\partial^2/\partial\theta^2$

From (6), we obtain

$$\left(\nabla^2 + (\alpha_1 a)^2\right)\phi_n = 0 \tag{8}$$

where $(\alpha_1 a)^2 = \left(\xi^2 + c^2\right)/\left(2+\overline{\lambda}\right)$. The solution of Eq.(8) for symmetric mode is

$$\phi_n = A_1 J_n\left(\alpha_1 a x\right)\cos n\theta \tag{9}$$

Similarly the solution for the anti symmetric mode $\overline{\phi}_n$ is obtained by replacing $\cos n\theta$ by $\sin n\theta$ in Eq.(9).

$$\overline{\phi}_n = \overline{A}_1 J_n\left(\alpha_1 a x\right)\sin n\theta \tag{10}$$

where J_n is the Bessel function of first kind of order n. Solving Eq.(7), we obtain

$$\psi_n = A_2 J_n\left(\alpha_2 a x\right)\sin n\theta \tag{11}$$

for symmetric mode and $\overline{\psi}_n$ is obtained from Eq.(11) by replacing $\sin n\theta$ by $\cos n\theta$, we get

$$\overline{\psi}_n = \overline{A}_2 J_n\left(\alpha_2 a x\right)\cos n\theta \tag{12}$$

for the anti symmetric mode. Here $(\alpha_2 a)^2 = \left(\xi^2 + c^2\right)$. If $(\alpha_i a)^2 < 0$, $i = 1,2$ then the Bessel function J_n of first kind is to be replaced by the modified Bessel function of the first kind I_n.

4. Solution of Fluid Medium

In cylindrical coordinates, the acoustic pressure and radial displacement equation of motion for an in viscid fluid are of the form Achenbach [21]

$$p^f = -B^f\left(u^f_{r,r} + r^{-1}\left(u^f_r + u^f_{\theta,\theta}\right)\right) \tag{13}$$

and

$$c_f^{-2}u^f_{r,tt} = \Delta_{,r} \tag{14}$$

respectly, where $\left(u^f_r, u^f_\theta\right)$ is the displacement vector, B^f is the adiabatic bulk modulus, $c_f = \sqrt{B^f/\rho^f}$ is the acoustic phase velocity of the fluid in which ρ^f is the density of the fluid and

$$\Delta = \left(u^f_{r,r} + r^{-1}\left(u^f_r + u^f_{\theta,\theta}\right)\right) \tag{15}$$

substituting $u^f_r = \phi^f_{,r}$ and $u^f_\theta = r^{-1}\phi^f_{,\theta}$ and seeking the solution of Eq.(14) in the form

$$\phi^f(r,\theta,t) = \sum_{n=0}^{\infty}\varepsilon_n\phi_n^f\cos n\theta e^{i\omega t} \tag{16}$$

where

$$\phi_n^f = A_3 H_n^{(1)}\left(\alpha_3 a x\right) \tag{17}$$

where $(\alpha_3 a)^2 = \xi^2/\overline{\rho^f}\,\overline{B^f}$ in which $\overline{\rho} = \rho/\rho^f$, $\overline{B^f} = B^f/\mu$, $H_n^{(1)}$ is the Hankel function of first kind of order n. If $(\alpha_3 a)^2 < 0$, then the Hankel function of first kind is replaced with K_n, where K_n is the modified Bessel function of second kind. Substituting the Eq. (16) in Eq. (13) along with the Eq. (17), we could express the acoustic pressure of the fluid as

$$p^f = \sum_{n=0}^{\infty}\varepsilon_n A_3\xi^2\overline{\rho}H_n^{(1)}\left(\alpha_3 a x\right)\cos n\theta e^{i\omega t} \tag{18}$$

5. Boundary Conditions and Frequency Equations

In this problem, the free vibration of a polygonal (triangle, square, pentagon and hexagon) cross sectional rotating plate immersed in fluid is considered. Since the boundary is irregular, it is difficult to satisfy the boundary conditions of the plate directly. Hence, in the same lines of Nagaya [1, 2], the Fourier expansion collocation method is applied to satisfy the boundary conditions. Thus the boundary conditions are obtained as

$$\left(\sigma_{xx} + p^f\right)_i = \left(\sigma_{xy}\right)_i = \left(u_r - u^f_r\right)_i = 0 \tag{19}$$

where x is the coordinate normal to the boundary and y is the tangential coordinate to the boundary, σ_{xx} is the normal stress, σ_{xy} is the shearing stress and $(\ )_i$ is the value at the i th segment of the boundary. The first and last conditions in equations (19) are due to the continuity of the stresses and displacements of the plate and fluid on the curved surface. If the angle γ_i between the normal to the segment and the reference axis is assumed to be constants, thus the transformed expression for the stresses is given by Nagaya [1, 2].

$$\sigma_{xx} = \lambda\left(u_{r,r} + r^{-1}\left(u_r + u_{\theta,\theta}\right)\right) + 2\mu[u_{r,r}\cos^2(\theta-\gamma_i) + r^{-1}\left(u_r + u_{\theta,\theta}\right)\sin^2(\theta-\gamma_i) + 0.5\left(r^{-1}\left(u_\theta - u_{r,\theta}\right) - u_{\theta,r}\right)\sin 2(\theta-\gamma_i)]$$

$$\sigma_{xy} = \mu[u_{r,r} - r^{-1}\left(u_{\theta,\theta} + u_r\right)\sin 2(\theta-\gamma_i) + \left(r^{-1}\left(u_{r,\theta} - u_\theta\right) + u_{\theta,r}\right)\sin 2(\theta-\gamma_i)] \tag{20}$$

The boundary conditions in Eq.(19) are transformed as

$$\left[\left(S_{xx}\right)_i + \left(\overline{S}_{xx}\right)_i\right]e^{i\xi T} = 0$$

$$\left[\left(S_{xy}\right)_i + \left(\overline{S}_{xy}\right)_i\right]e^{i\xi T} = 0$$

$$\left[\left(S_r\right)_i + \left(\overline{S}_r\right)_i\right]e^{i\xi T} = 0 \tag{21}$$

where

$$S_{xx} = 0.5\left(x_0^1 A_{10} + x_0^2 A_{20}\right) + \sum_{n=1}^{\infty}\left(x_n^1 A_{1n} + x_n^2 A_{2n} + x_n^3 A_{3n}\right)$$

$$S_{xy} = 0.5\left(y_0^1 A_{10} + y_0^2 A_{20}\right) + \sum_{n=1}^{\infty}\left(y_n^1 A_{1n} + y_n^2 A_{2n} + y_n^3 A_{3n}\right)$$

$$S_t = 0.5\left(z_0^1 A_{10} + z_0^2 A_{20}\right) + \sum_{n=1}^{\infty}\left(z_n^1 A_{1n} + z_n^2 A_{2n} + z_n^3 A_{3n}\right) \tag{22}$$

$$\overline{S}_{xx} = 0.5\left(\overline{x}_0^3 \overline{A}_{30}\right) + \sum_{n=1}^{\infty}\left(\overline{x}_n^1 \overline{A}_{1n} + \overline{x}_n^2 \overline{A}_{2n} + \overline{x}_n^3 \overline{A}_{3n}\right)$$

$$\overline{S}_{xy} = 0.5\left(\overline{x}_0^3 \overline{A}_{30}\right) + \sum_{n=1}^{\infty}\left(\overline{x}_n^1 \overline{A}_{1n} + \overline{x}_n^2 \overline{A}_{2n} + \overline{x}_n^3 \overline{A}_{3n}\right)$$

$$\overline{S}_t = 0.5\left(\overline{z}_0^3 \overline{A}_{30}\right) + \sum_{n=1}^{\infty}\left(\overline{z}_n^1 \overline{A}_{1n} + \overline{z}_n^2 \overline{A}_{2n} + \overline{z}_n^3 \overline{A}_{3n}\right) \tag{23}$$

The coefficients for $x_n^i \sim \overline{z}_n^i, i = 1,2,3$ are given in the Appendix A.

Performing the Fourier series expansion to Eq.(19) along the boundary, the boundary conditions are expanded in the form of double Fourier series. For the symmetric mode, the boundary conditions are expressed as follows.

$$\sum_{m=0}^{\infty}\varepsilon_m\left[X_{m0}^1 A_{10} + X_{m0}^2 A_{20} + \sum_{n=1}^{\infty}\left(X_{mn}^1 A_{1n} + X_{mn}^2 A_{2n} + X_{mn}^3 A_{3n}\right)\right]\cos m\theta = 0$$

$$\sum_{m=1}^{\infty}\left[Y_{m0}^1 A_{10} + Y_{m0}^2 A_{20} + \sum_{n=1}^{\infty}\left(Y_{mn}^1 A_{1n} + Y_{mn}^2 A_{2n} + Y_{mn}^3 A_{3n}\right)\right]\sin m\theta = 0$$

$$\sum_{m=0}^{\infty} \varepsilon_m \left[Z_{m0}^1 A_{10} + Z_{m0}^2 A_{20} + \sum_{n=1}^{\infty} \left(Z_{mn}^1 A_{1n} + Z_{mn}^2 A_{2n} + Z_{mn}^3 A_{3n} \right) \right] \cos m\theta = 0 \tag{24}$$

Similarly, for antisymmetric mode, the boundary conditions are expressed as

$$\sum_{m=1}^{\infty} \left[\overline{X}_{m0}^3 \overline{A}_{30} + \sum_{n=1}^{\infty} \left(\overline{X}_{mn}^1 \overline{A}_{1n} + \overline{X}_{mn}^2 \overline{A}_{2n} + \overline{X}_{mn}^3 \overline{A}_{3n} \right) \right] \sin m\theta = 0$$

$$\sum_{m=0}^{\infty} \varepsilon_m \left[\overline{Y}_{m0}^3 \overline{A}_{30} + \sum_{n=1}^{\infty} \left(\overline{Y}_{mn}^1 \overline{A}_{1n} + \overline{Y}_{mn}^2 \overline{A}_{2n} + \overline{Y}_{mn}^3 \overline{A}_{3n} \right) \right] \cos m\theta = 0$$

$$\sum_{m=1}^{\infty} \left[\overline{Z}_{m0}^3 \overline{A}_{30} + \sum_{n=1}^{\infty} \left(\overline{Z}_{mn}^1 \overline{A}_{1n} + \overline{Z}_{mn}^2 \overline{A}_{2n} + \overline{Z}_{mn}^3 \overline{A}_{3n} \right) \right] \sin m\theta = 0 \tag{25}$$

where

$$X_{mn}^j = \left(2\varepsilon_n/\pi\right) \sum_{i=1}^{I} \int_{\theta_{i-1}}^{\theta_i} x_n^j \left(R_i, \theta\right) \cos m\theta d\theta$$

$$Y_{mn}^j = \left(2\varepsilon_n/\pi\right) \sum_{i=1}^{I} \int_{\theta_{l-1}}^{\theta_l} y_n^j \left(R_i, \theta\right) \sin m\theta d\theta$$

$$Z_{mn}^j = \left(2\varepsilon_n/\pi\right) \sum_{i=1}^{I} \int_{\theta_{i-1}}^{\theta_i} z_n^j \left(R_i, \theta\right) \cos m\theta d\theta \tag{26}$$

$$\overline{X}_{mn}^j = \left(2\varepsilon_n/\pi\right) \sum_{i=1}^{I} \int_{\theta_{i-1}}^{\theta_i} \overline{x}_n^j \left(R_i, \theta\right) \sin m\theta d\theta$$

$$\overline{Y}_{mn}^j = \left(2\varepsilon_n/\pi\right) \sum_{i=1}^{I} \int_{\theta_{l-1}}^{\theta_l} \overline{y}_n^j \left(R_i, \theta\right) \cos m\theta d\theta$$

$$\overline{Z}_{mn}^j = \left(2\varepsilon_n/\pi\right) \sum_{i=1}^{I} \int_{\theta_{i-1}}^{\theta_i} \overline{z}_n^j \left(R_i, \theta\right) \sin m\theta d\theta \tag{27}$$

where $j = 1, 2$, and 3, I is the number of segments, R_i is the coordinate r at the boundary and N is the number of truncation of the Fourier series. The frequency equations are obtained by truncating the series to $N+1$ terms, and equating the determinant of the coefficients of the amplitude $A_{in} = 0$ and $\overline{A}_{in} = 0$, for symmetric and antisymmetric modes of vibrations. Thus, the frequency equation for the symmetric mode is obtained from Eq. (24), by equating the determinant of the coefficient matrix of $A_{in} = 0$. Therefore we have

$$\begin{bmatrix} X_{00}^1 & X_{00}^2 & X_{01}^1 & \cdots & X_{0N}^1 & X_{01}^2 & \cdots & X_{0N}^2 & X_{01}^3 & \cdots & X_{0N}^3 \\ \vdots & \vdots & \vdots & & \vdots & \vdots & & \vdots & \vdots & & \vdots \\ X_{N0}^1 & X_{N0}^2 & X_{N1}^1 & \cdots & X_{NN}^1 & X_{N1}^2 & \cdots & X_{NN}^2 & X_{N1}^3 & \cdots & X_{NN}^3 \\ Y_{00}^1 & Y_{00}^2 & Y_{01}^1 & \cdots & Y_{0N}^1 & Y_{01}^2 & \cdots & Y_{0N}^2 & Y_{01}^3 & \cdots & Y_{0N}^3 \\ \vdots & \vdots & \vdots & & \vdots & \vdots & & \vdots & \vdots & & \vdots \\ Y_{N0}^1 & Y_{N0}^2 & Y_{N1}^1 & \cdots & Y_{NN}^1 & Y_{N1}^2 & \cdots & Y_{NN}^2 & Y_{N1}^3 & \cdots & Y_{NN}^3 \\ Z_{00}^1 & Z_{00}^2 & Z_{01}^1 & \cdots & Z_{0N}^1 & Z_{01}^2 & \cdots & Z_{0N}^2 & Z_{01}^3 & \cdots & Z_{0N}^3 \\ \vdots & \vdots & \vdots & & \vdots & \vdots & & \vdots & \vdots & & \vdots \\ Z_{N0}^1 & Z_{N0}^2 & Z_{N1}^1 & \cdots & Z_{NN}^1 & Z_{N1}^2 & \cdots & Z_{NN}^2 & Z_{N1}^3 & \cdots & Z_{NN}^3 \end{bmatrix} \begin{bmatrix} A_{10} \\ A_{20} \\ A_{11} \\ \vdots \\ A_{1N} \\ \vdots \\ A_{31} \\ \vdots \\ A_{3N} \end{bmatrix} = 0 \tag{28}$$

Similarly, the frequency equation for antisymmetric mode is obtained from the Eq. (25) by equating the determinant of the coefficient matrix of $\overline{A}_{in}$ to zero. Therefore, for the antisymmetric mode, the frequency equation is obtained as

$$\begin{bmatrix} \overline{X}_{10}^3 & \overline{X}_{11}^1 & \cdots & \overline{X}_{1N}^1 & \overline{X}_{11}^2 & \cdots & \overline{X}_{1N}^2 & \overline{X}_{11}^3 & \cdots & \overline{X}_{1N}^3 \\ \vdots & \vdots & & \vdots & \vdots & & \vdots & \vdots & & \vdots \\ \overline{X}_{N0}^3 & \overline{X}_{N1}^1 & \cdots & \overline{X}_{NN}^1 & \overline{X}_{N1}^2 & \cdots & \overline{X}_{NN}^2 & \overline{X}_{N1}^3 & \cdots & \overline{X}_{NN}^3 \\ \overline{Y}_{10}^3 & \overline{Y}_{11}^1 & \cdots & \overline{Y}_{1N}^1 & \overline{Y}_{11}^2 & \cdots & \overline{Y}_{1N}^2 & \overline{Y}_{11}^3 & \cdots & \overline{Y}_{1N}^3 \\ \vdots & \vdots & & \vdots & \vdots & & \vdots & \vdots & & \vdots \\ \overline{Y}_{N0}^3 & \overline{Y}_{N1}^1 & \cdots & \overline{Y}_{NN}^1 & \overline{Y}_{N1}^2 & \cdots & \overline{Y}_{NN}^2 & \overline{Y}_{N1}^3 & \cdots & \overline{Y}_{NN}^3 \\ \overline{Z}_{10}^3 & \overline{Z}_{11}^1 & \cdots & \overline{Z}_{1N}^1 & \overline{Z}_{11}^2 & \cdots & \overline{Z}_{1N}^2 & \overline{Z}_{11}^3 & \cdots & \overline{Z}_{1N}^3 \\ \vdots & \vdots & & \vdots & \vdots & & \vdots & \vdots & & \vdots \\ \overline{Z}_{N0}^3 & \overline{Z}_{N1}^1 & \cdots & \overline{Z}_{NN}^1 & \overline{Z}_{N1}^2 & \cdots & \overline{Z}_{NN}^2 & \overline{Z}_{N1}^3 & \cdots & \overline{Z}_{NN}^3 \end{bmatrix} \begin{bmatrix} \overline{A}_{31} \\ \overline{A}_{11} \\ \vdots \\ \overline{A}_{1N} \\ \overline{A}_{21} \\ \vdots \\ \overline{A}_{2N} \\ \overline{A}_{31} \\ \vdots \\ \overline{A}_{3N} \end{bmatrix} = 0 \tag{29}$$

6. Numerical Results and Discussions

The numerical analysis of the frequency equation is carried out for rotating polygonal (square, triangle, pentagon and hexagon) cross-sectional plates immersed in fluid, and the dimensions of each plate used in the numerical calculation are shown in Figure 1, and its geometric relations for the polygonal cross-sections given by Nagaya [1, 2] as

$$R_i / b = \left[\cos\left(\theta - \gamma_i\right)\right]^{-1} \tag{30}$$

where b is the apothem. The relation given in Eq. (30) is used directly for the numerical calculation. The axis of symmetry is denoted by the lines in the figures. where b is the apothem.

The frequency equations are obtained in symmetric and anti symmetric cases given in equations (28) and (29) are analyzed numerically for rotating plate of triangular, square, pentagonal and hexagonal cross sections immersed in fluid. The material properties used for the computation are as follows: For the solid the Poisson ratio $\nu = 0.3$, density $\rho = 7849 kg / m^3$ and the Young's modulus $E = 2.139 \times 10^{11} N / m^2$ and for the fluid: the density $\rho^f = 1000 Kg / m^3$ and the phase velocity $c = 1500 m / s$. The dimensionless frequencies are computed using Secant method (applicable for complex roots [9]) for polygonal cross sectional rotating plate immersed in fluid. The polygonal cross sectional plate in the range $\theta = 0$ and $\theta = \pi$ is divided into many segments for convergence of frequency in such a way that the distance between any two segments is negligible. Integration is performed for each segment numerically by use of Gauss Gauss five point formula .The non-dimensional frequencies are computed for $0 < \Omega \le 1.0$, using the secant method.

6.1. Rotating Polygonal cross-sectional Plates

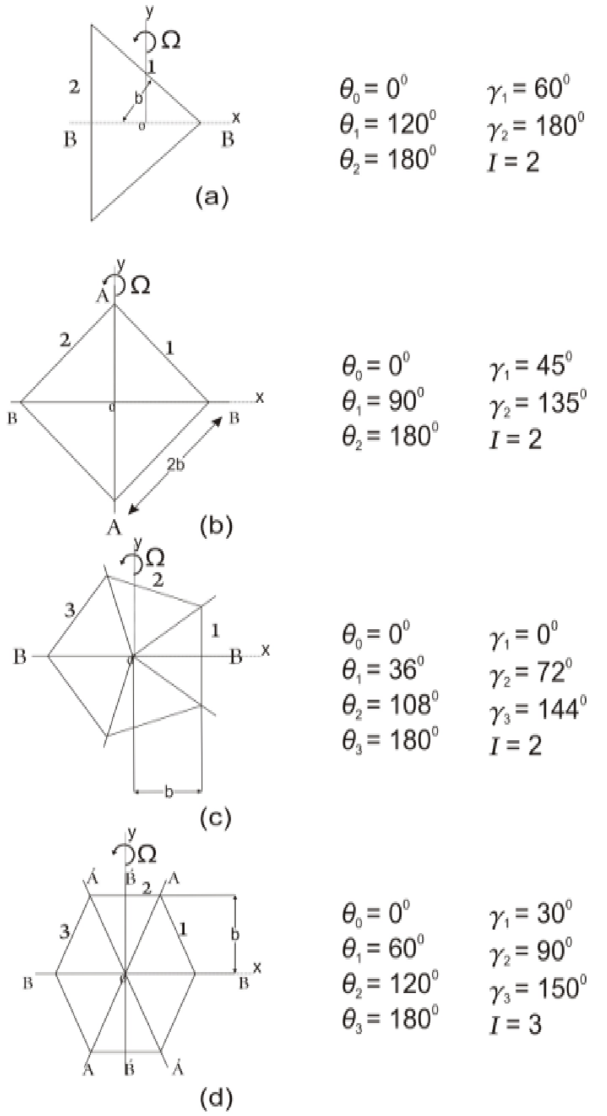

Figure 1. Rotating Plate of Polygonal cross-sections. (a) Triangle (b) Square (c) Pentagon (d) Hexagon

6.1.1. Square and Hexagonal cross-sectional Plate

In the case of longitudinal vibration of square and hexagonal cross sectional plates, the displacements are symmetrical about both major and minor axes since both the cross sections are symmetrical about both the axes. Therefore the frequency equation is obtained by choosing both terms of n and m are chosen as $0,2,4,6,...$ in Eq. (28) . During flexural motion, the displacements are anti symmetrical about the major axis and symmetrical about the minor axis. Hence the frequency equation is obtained by choosing $n,m=1,3,5,...$ in Eq. (29).

6.1.2. Triangle and Pentagonal Cross-sectional Plate

The triangular and pentagonal cross sectional plate, the vibration displacements are symmetrical about the major axis for the longitudinal mode and anti symmetrical about the minor axis for the flexural mode since the cross section is symmetric about only one axis. Therefore n and m are chosen as $0,1,2,3,...$ in Eq. (28) for longitudinal mode and $n,m=1,2,3,...$ in Eq. (29) for the flexural anti symmetric mode.

6.1.3. Dispersion Curves

A graph is drawn between the rotational speeds of $\Omega = 0.5$ and non-dimensional frequency of longitudinal modes of a triangular cross-sectional plate in space, immersed in fluid and rotating plate immersed in fluid and is shown in Fig. 2. From Fig. 2, it is observed that as mode increases the dimensionless frequencies increases. Also it is observed that the dimensionless frequencies of plate in space are higher than the plate immersed in fluid and rotating plate immersed in fluid. The dimensionless frequencies of rotating plate immersed in fluid increases and decreases as mode increases.

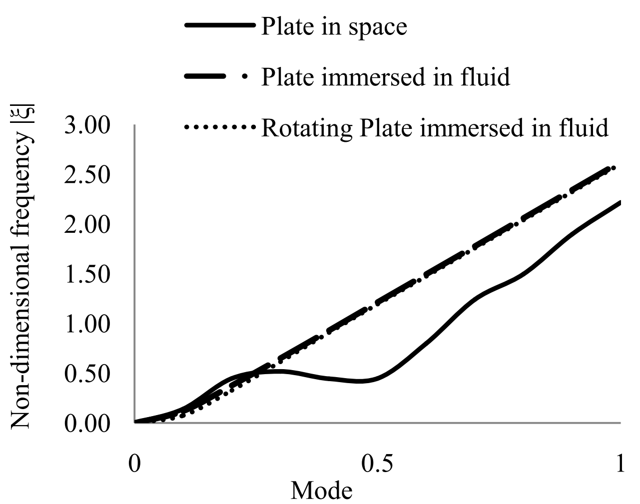

Figure 2. Comparison between the frequency response of longitudinal modes of triangular cross-sectional plate in space, immersed in fluid and rotating with a speed of Ω=0.5

A graph is drawn between the rotational speed and non-dimensional frequency $|\xi|$ of longitudinal modes of triangular cross-sectional plate immersed in fluid and is shown in Fig. 3. From Fig. 3, it is observed that as mode increases the non-dimensional frequency increases. Further it is observed that as rotational speed increases the dimensional frequencies increases.

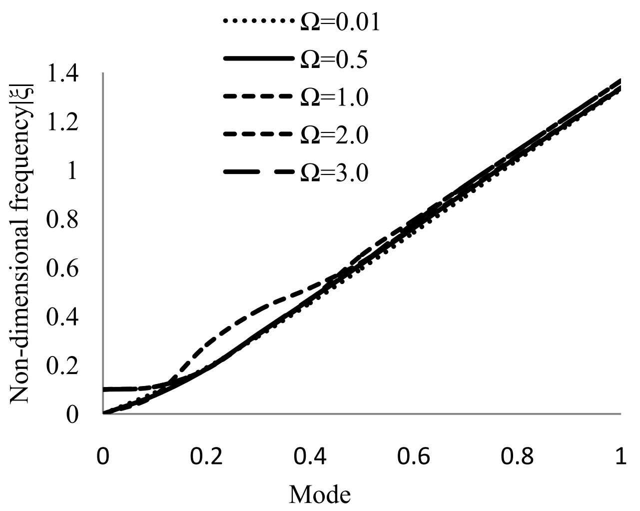

Figure 3. Rotational speed versus non-dimensional frequency |ξ| of longitudinal modes of triangular cross-sectional plate immersed in fluid

Graph is drawn between the mode and non-dimensional frequency $|\xi|$ for flexural antisymmetric modes of triangular cross-sectional rotating plate immersed in fluid and is shown in Fig. 4. From Fig. 4, it is observed that as mode increases both the real and imaginary part of non-dimensional frequencies increases. It is interesting to note that the real part of dimensional frequencies is higher than that of the imaginary part as rotation increases.

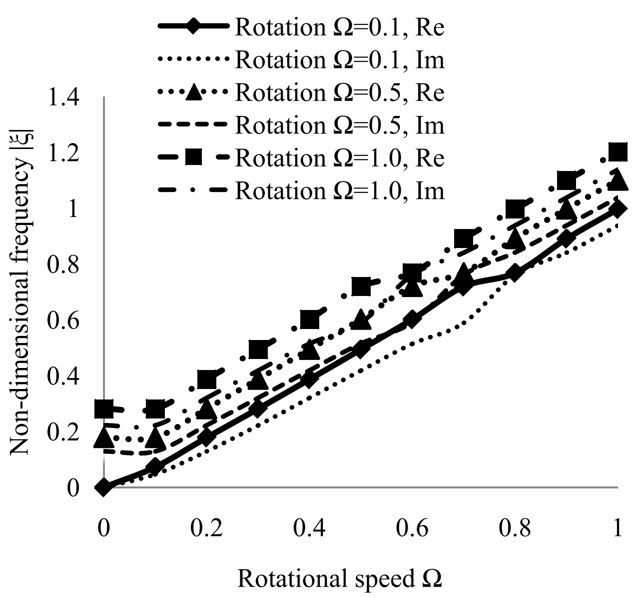

Figure 4. Rotational speed Ω=0.1, 0.5, 1.0 versus dimensionaless frequency |ξ| for a flexural antisymmetric modes of triangular cross-sectional rotating plate immersed in fluid

Graphs are drawn between mode and non-dimensional frequency $|\xi|$ for longitudinal modes of square and hexagonal cross-sectional rotating plate immersed in plate and are is shown in Figs. 5 and 6. From Figs. 5 and 6, it is observed that the dimensional frequencies increases as rotating speed increases. Also it is observed that the cross over points in the trend lines denote the transfer of energy between the modes of vibration.

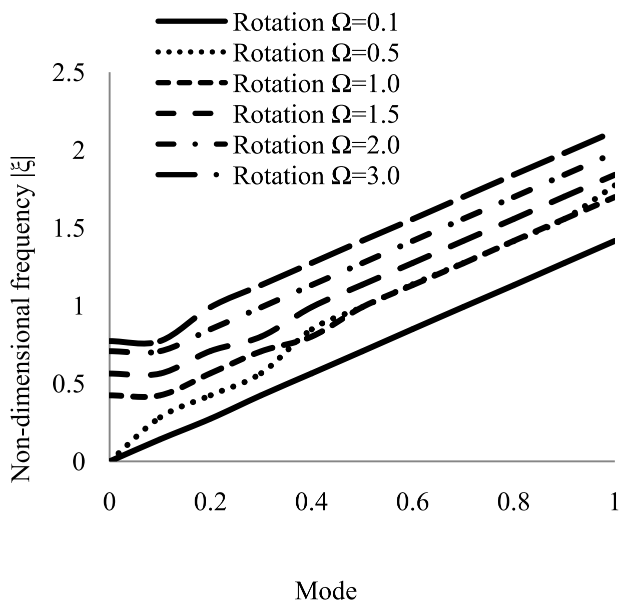

Figure 5. Rotational speed Ω=0.1, 0.5, 1.0, 2.0 and 3.0versus dimensionaless frequency |ξ| for longitudinal modes of square cross-sectional rotating plate immersed in fluid

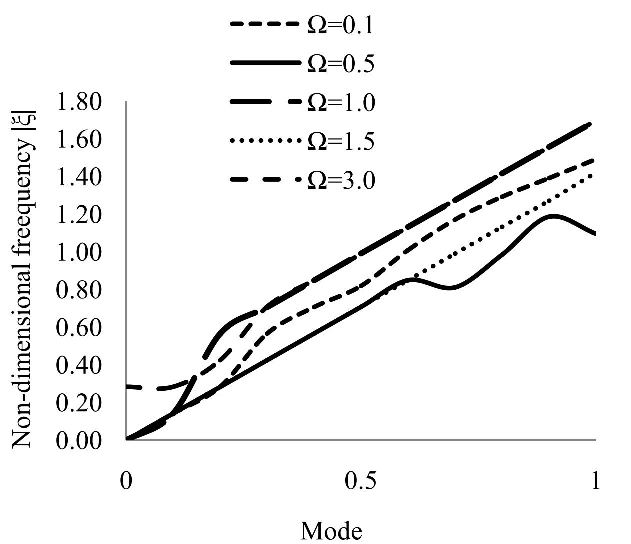

Figure 6. Rotational speed versus non-dimensional frequency |ξ| of longitudinal modes of hexagonal cross-sectional plate immersed in fluid

A graph is drawn between the mode and non-dimensional frequency for different longitudinal modes of pentagonal cross-sectional plate immersed in fluid with fixed rotational speed $\Omega = 0.1$ and is shown in Fig. 7. From Fig. 7, it is observed that as mode increases the non-dimensional frequency increases. The notation Lm denotes for longitudinal modes of vibration. Also it is noted that as longitudinal modes of vibration increases the non-dimensional frequency increases.

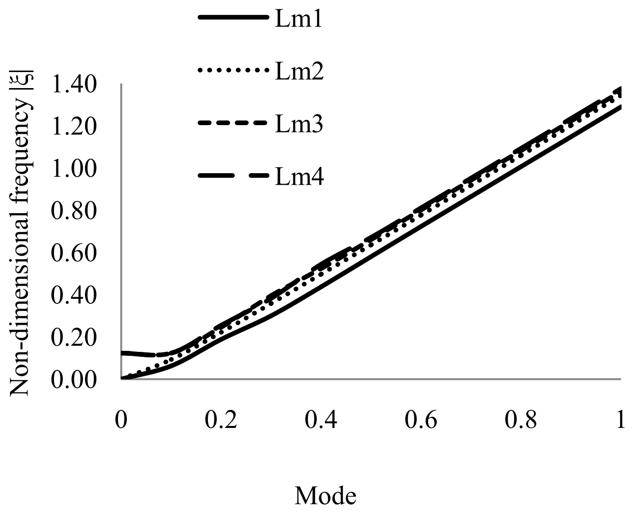

Figure 7. Rotation Ω=0.1, the frequency response for different longitudinal modes of pentagonal cross-sectional plate immersed in fluid

5. Conclusions

In this paper, a method for solving the wave propagation problem of rotating polygonal cross sectional plate immersed in fluid has been presented. The frequency equation has obtained using Fourier expansion collocation method. Numerical calculations have been carried out for triangular, square, pentagonal and hexagonal cross sectional rotating plate immersed in fluid. This method is straightforward and the numerical results for any other polygonal cross section can be obtained directly for the same frequency equation by substituting geometric values of the boundary of any cross section analytically or numerically with satisfactory convergence.

Appendix A

$$e^{1}_{n} = 2\left\{n(n-1)J_n(\alpha_1 ax)+(\alpha_1 ax)J_{n+1}(\alpha_1 ax)\right\}\cos 2(\theta-\gamma_l)\cos n\theta$$
$$-x^2\left\{(\alpha_1 a)^2\left(\bar{\lambda}+2\cos^2(\theta-\gamma_l)\right)\right\}J_n(\alpha_1 ax)\cos n\theta$$

$$\bar{e}^{1}_{n} = 2\left\{n(n-1)J_n(\alpha_1 ax)+(\alpha_1 ax)J_{n+1}(\alpha_1 ax)\right\}\cos 2(\theta-\gamma_l)\sin n\theta$$
$$-x^2\left\{(\alpha_1 a)^2\left(\bar{\lambda}+2\cos^2(\theta-\gamma_l)\right)\right\}J_n(\alpha ax)\sin n\theta$$

$$e^{2}_{n} = 2n\left\{(n-1)J_n(\alpha_2 ax)+(\alpha_2 ax)J_{n+1}(\alpha_2 ax)\right\}\cos 2(\theta-\gamma_l)\cos n\theta$$
$$+2\left\{\left(n(n-1)-(\alpha_2 ax)^2\right)J_n(\alpha_2 ax)+(\alpha_2 ax)J_{n+1}(\alpha_2 ax)\right\}\sin 2(\theta-\gamma_l)\sin n\theta$$

$$\bar{e}^{2}_{n} = 2n\left\{(n-1)J_n(\alpha_2 ax)+(\alpha_2 ax)J_{n+1}(\alpha_2 ax)\right\}\cos 2(\theta-\gamma_l)\sin n\theta$$
$$-2\left\{\left(n(n-1)-(\alpha_2 ax)^2\right)J_n(\alpha_2 ax)+(\alpha_2 ax)J_{n+1}(\alpha_2 ax)\right\}\sin 2(\theta-\gamma_l)\cos n\theta$$

$$e^{3}_{n} = \xi^2\bar{\rho}H^{(1)}_{n}(\alpha_3 ax)\cos n\theta$$
$$\bar{e}^{3}_{n} = \xi^2\bar{\rho}H^{(1)}_{n}(\alpha_3 ax)\sin n\theta$$

$$f^{1}_{n} = 2\left\{n(n-1)-(\alpha_1 ax)^2 J_n(\alpha_1 ax)+(\alpha_1 ax)J_{n+1}(\alpha_1 ax)\right\}\sin 2(\theta-\gamma_l)\cos n\theta$$
$$+2n\left\{(\alpha_1 ax)J_{n+1}(\alpha_1 ax)-(n-1)J_n(\alpha_1 ax)\right\}\cos 2(\theta-\gamma_l)\sin n\theta$$

$$\overline{f}^1_n = 2\left\{n(n-1)-(\alpha_1 ax)^2 J_n(\alpha_1 ax)+(\alpha_1 ax)J_{n+1}(\alpha_1 ax)\right\}\sin 2(\theta-\gamma_l)\sin n\theta$$
$$-2n\left\{(\alpha_1 ax)J_{n+1}(\alpha_1 ax)-(n-1)J_n(\alpha_1 ax)\right\}\cos 2(\theta-\gamma_l)\cos n\theta$$

$$f^3{}_n = 2n\left\{(n-1)J_n(\alpha_2 ax)-(\alpha_2 ax)J_{n+1}(\alpha_2 ax)\right\}\sin 2(\theta-\gamma_l)\cos n\theta$$
$$+2\left\{(\beta ax)J_{n+1}(\alpha_2 ax)-\left(n(n-1)-(\alpha_2 ax)^2\right)J_n(\alpha_2 ax)\right\}\cos 2(\theta-\gamma_l)\sin n\theta$$

$$\overline{f}^3_n = 2n\left\{(n-1)J_n(\alpha_2 ax)-(\alpha_2 ax)J_{n+1}(\alpha_2 ax)\right\}\sin 2(\theta-\gamma_l)\sin n\theta$$
$$-2\left\{(\alpha_2 ax)J_{n+1}(\alpha_2 ax)-\left(n(n-1)-(\alpha_2 ax)^2\right)J_n(\alpha_2 ax)\right\}\cos 2(\theta-\gamma_l)\cos n\theta$$

$$g^1{}_n = \left\{nJ_n(\alpha_1 ax)-(\alpha_1 ax)J_{n+1}(\alpha_1 ax)\right\}\cos n\theta$$

$$\overline{g}^1_n = \left\{nJ_n(\alpha_1 ax)-(\alpha_1 ax)J_{n+1}(\alpha_1 ax)\right\}\sin n\theta$$

$$g^2{}_n = nJ_n(\alpha_2 ax)\cos n\theta$$

$$\overline{g}^2_n = nJ_n(\alpha_2 ax)\sin n\theta$$

$$g^3{}_n = -\left[nH_n^{(1)}(\alpha_3 ax)-(\alpha_3 ax)H_{n+1}^{(1)}(\alpha_3 ax)\right]\cos n\theta$$

$$\overline{g}^3_n = -\left[nH_n^{(1)}(\alpha_3 ax)-(\alpha_3 ax)H_{n+!}^{(1)}(\alpha_3 ax)\right]\sin n\theta$$

REFERENCES

[1] Nagaya, K., 1981, Simplified Method for solving problems of vibrating plates of doubly connected arbitrary shape Part I: Derivation of the frequency equation, J. Sound and Vib., 74(4), 543-551.

[2] Nagaya, K., 1981, Simplified method for solving problem of vibrating plates of doubly connected arbitrary shape Part II: Applications and experiments, J. Sound and Vib., 74(4), 553-564.

[3] Ponnusamy, P., 2007, Wave propagation in a generalized thermo elastic solid cylinder of arbitrary cross-section, Int. J. Solid and Struct., 44, 5336-5348.

[4] Ponnusamy, P., 2011, Wave propagation in thermo-elastic plate of arbitrary cross-sections, J. Multidiscipline Modelling in Materials and Structures, 7(3), 329-350.

[5] Ponnusamy, P., 2012, Dispersion analysis of generalized thermo elastic plate of polygonal cross-sections, J. Appl. Mathematical Modeling, 36, 3343-3358.

[6] Ponnusamy, P., 2013, Wave propagation in a piezoelectric solid bar of circular cross-section immersed in fluid, Int. J. Pressure Vessels and Piping, 105-106, 12-18.

[7] Clarke, N. S., and Burdess, J. S., 1994, A rotation rate sensor based upon a Rayleigh resonator, J. Appl. Mech. ASME, 61, 139-143.

[8] Wren, T., and Burdess, J. S., 1987, Surface waves perturbed by rotation, J. Appl. Mech. ASME, 54, 464-468.

[9] Soderkvist, J., 1994, Micro Machined gyroscopes, Sensor and Actuators A, 43, 65-71.

[10] Ting, T.C.T., 2004, Surface waves in rotating anisotropic elastic half space, Wave motion, 40, 329-346.

[11] Stroh, A.N., 1962, Steady state problem in anisotropic elasticity, J. Math. Phys., 41, 77-103.

[12] Fang, H. Y., Yang, J. S., and Jiang, Q., 2000, Rotation sensitivity of waves propagating in a piezoelectric plate, Int. J. Solid Structures, 39, 5241-5251.

[13] Fang, H. Y., Yang, J. S., and Jiang, Q., 2002, Rotation perturbed surface acoustic waves propagating in piezoelectric crystals, Int. J. Solid Structures, 37, 4933-4947.

[14] Sharma, J. N., and Thakur, M., 2006, Effect of rotation on Rayleigh Lamb waves in magneto-thermo elastic media, J. Sound and Vib., 296, 871-881.

[15] Sharma, J. N., and Othman, I. A., 2007, Effect of rotation on generalized thermo-viscoelastic Rayleigh-Lamb waves, Int. J. Solid Structures, 44, 4243-4255.

[16] Walia, V., Sharma, J. N., and Sharma, P.K., 2009, Propagation characteristics of thermoelastic waves in piezoelectric (6mm class) rotating plate, European J. of Mechanics A/solids, 28, 569-581.

[17] Sun, J., Du, J., Yang, J., and Wang, J., 2012, Shear-horizontal waves in a rotated Y-cut quartz plate in contace with a viscous fluid, Ultrasonics, 52, 133-137.

[18] Assaf, S., Guerich, M., and Cuvelier, P., 2010, Vibration and acoustic response of damped sandwich plates immersed in a light or heavy fluid, Computer and Structures, 88, 870-878.

[19] Ahmed Shah, S., and Tajuddin, M., 2011, Three dimensional vibration analysis of an infinite poroelastic plate immersed in an inviscid elastic fluid, Int. J. Engg. Sci and Tech., 3(2), 1-11.

[20] Mirsky, I., 1964, Wave propagation in a transversely isotropic circular cylinders Part I: Theory; Part II: Numerical results, J. Acoustical Society of America, 37(6), 1016-1026.

[21] Achenbach, J. D., 1973, Wave propagation in elastic solids, Elsevier Publishing Company Inc., New York.